



Metal–insulator transition in the high pressure cubic CaF_2 -type structure of CrO_2

S BISWAS[✉]

Department of Physics, Taki Government College, Taki, North 24 Parganas 743429, India
srisabuj.phys@gmail.com

MS received 29 April 2017; accepted 9 June 2017; published online 22 March 2018

Abstract. The total energy, magnetic moment, density of states and energy band structures of CrO_2 in the high pressure cubic CaF_2 (Fm-3m)-type structure are investigated for the first time by using first principles electronic structure calculations based on density functional theory in the local spin density approximation (LSDA) as well as using LSDA + U method. It is revealed from the present study that CrO_2 is a ferromagnetic nearly half-metal in the LDA calculation due to almost occupied Cr-3d_{eg} orbitals in the spin majority species and a tiny electron contribution at the Fermi level (E_F) for spin minority species. This compound encounters metal–insulator transition (MIT) upon the application of Hubbard-type Coulomb repulsion $U = 1$ eV. Ferromagnetism is preserved in this transition. Application of U increases the electron correlation, which polarizes e_g orbitals far below E_F for spin majority channel while in the spin minority channel e_g orbitals are polarized well above E_F , resulting in opening of a band gap ($E_g \sim 1.05$ eV) in the vicinity of E_F . Coulomb repulsion increases hybridization between occupied Cr-3d_{eg} and O-2p orbitals, which induces ferromagnetism both in half-metallic and insulating phases of cubic CrO_2 .

Keywords. Half-metal; metal–insulator transition; double exchange mechanism; transition metal oxides; Coulomb interaction.

1. Introduction

Among the transition metal oxides (TMOs), chromium dioxide (CrO_2) as a candidate of strongly correlated electron system has attracted renewed interest in recent years due to its unusual electronic structure and magnetic properties [1–5]. In room temperature, this compound has tetragonal structure of rutile type exhibiting half-metallic ferromagnetic (HMF) behaviour with very high $T_c \approx 390$ K compared to other TMO candidates. These two properties along with its wide availability in nature make CrO_2 significantly and technologically important and ideal material for developing spintronic devices. It is the only stoichiometric binary compound which has HMF nature [6] at room temperature. CrO_2 turns into a very suitable and promising material for applications in devices based on tunnelling magneto-resistance with a favourable switching behaviour at small fields [4,7–9] and intergrain-tunnelling magneto-resistance [10–12] due to its HM property. As a result, with multiple industrial applications and due to its unusual HMF behaviour, CrO_2 has been extensively studied both theoretically and experimentally [13–22]. Under ambient conditions CrO_2 crystallizes in the rutile type (space group $P4_2/mnm$) structure, which is commonly found in metal oxides TiO_2 , ZrO_2 , VO_2 , SnO_2 , GeO_2 , RuO_2 etc. At high pressures, however, the electronic and magnetic properties as well as the physical properties of CrO_2 change significantly. Therefore,

investigation of physical properties of CrO_2 under high pressure and temperature has turned into an exceptionally important issue in recent years. The high pressure behaviour of CrO_2 has been extensively studied in a series of investigations [23–29].

Using angle resolved synchrotron X-ray diffraction and high sensitivity confocal Raman spectroscopy, Maddox *et al* [23] reported that rutile-type CrO_2 (tetragonal CrO_2 or t- CrO_2) transforms into orthorhombic CaCl_2 -type structure (o- CrO_2 in the space group Pnnm) under a pressure of 12 ± 3 GPa without any discontinuity in volume. Employing tight-binding linear muffin tin orbital (TB-LMTO) method, Srivastava *et al* [24] confirmed a structural phase transition (SPT) from t- CrO_2 to o- CrO_2 at 9.6 GPa and a pressure-induced magnetic phase transition from ferromagnetic to nonmagnetic (NM) at 65 GPa. They also reported a second SPT from o- CrO_2 to cubic CaF_2 -type (c- CrO_2 in the space group Fm-3m) at a pressure 89.6 GPa with a volume collapse of 7.3%. According to their report, half-metallicity was preserved in the transition from t- CrO_2 to o- CrO_2 , which vanishes at a pressure $P = 41.6$ GPa, whereas ferromagnetism (FM) is quenched at 65 GPa. However, they have not studied the electronic, magnetic or structural properties of c- CrO_2 .

In their study, Sooran *et al* [26] reported three possible SPTs with increasing pressure. The first transition from t- CrO_2 to o- CrO_2 was observed at pressure $P \approx 10$ GPa preserving FM and HM properties. At pressure $P \geq 61.1$ GPa, the second

SPT from FM o-CrO₂ to NM monoclinic CrO₂ (m-CrO₂ in the space group P2₁/c) of MoO₂ type was reported. The third transition from m-CrO₂ to c-CrO₂ was detected at 88.8 GPa. They demonstrated that c-CrO₂ is a FM insulator (FI) which is maintained up to 88.8 GPa. Wu *et al* [27] determined the SPTs t-CrO₂ to o-CrO₂, pyrite-type and c-CrO₂ at the phase transition pressures 10.9, 23.9 and 144.5 GPa respectively. Li and Hao [28] reported that t-CrO₂ transforms to PbO₂-type and pyrite-type structures at pressures 35.5 and 45 GPa respectively. Using *ab initio* constant pressure technique, Alptekin [29] demonstrated SPTs from t-CrO₂ to o-CrO₂ and o-CrO₂ to m-CrO₂ at pressures 30 and 35 GPa respectively.

Although the cubic CrO₂ of CaF₂-type structure was discovered by Sooran *et al*, there is no report till now to explore its electronic and magnetic properties. In this paper, the electronic and magnetic properties of c-CrO₂ are investigated extensively. In the ongoing work, it is observed for the first time that c-CrO₂ is a FM nearly half-metal (NHM) but still metallic in the local spin density approximations (LSDA) contrasting to the report of Sooran *et al* [26]. The HM behaviour of c-CrO₂ is very exceptional comparing to that of t-CrO₂. For t-CrO₂, the majority spin species are metallic and the minority spin species are insulating, but in case of c-CrO₂ the majority spin species are insulating while the minority spins species are metallic with minute contribution of charge carriers at E_F. However, this material in its cubic structure encounters metal-insulator transition (MIT) upon the application of Coulomb repulsion $U = 1$ eV preserving FM behaviour in the insulating state. This is very unusual because ferromagnetism (FM) is accompanied by metallicity and insulating TMOs are usually antiferromagnetic. In the present study, concentration has been paid to investigate the origin of MIT of CrO₂ in the cubic CaF₂-type structure.

2. Method of calculations

The total energy, band structure (BS), densities of states (DOS) and structural analysis of c-CrO₂ were carried out in the FM state, using density functional theory (DFT) [30,31] implemented in the tight-binding linear muffin-tin orbital (TB-LMTO) method in its atomic sphere approximation (ASA) [32,33]. Local spin density approximations (LSDA) [33,34] were used for the electronic structure calculations of c-CrO₂. The LSDA is well known to fail to predict the exact ground-state electronic properties of most of the 3d metal oxides. In this respect, the LSDA + U scheme [35,36], which includes explicitly an on-site correlation term, has brought exceptional improvement in the description of most of the 3d metal oxides, because it correctly yields the insulating ground-state properties. To understand the underlying physics behind the MIT in c-CrO₂, LSDA + U calculations have been carried out for exact description of ground-state properties. Self-consistent electronic structure calculations were performed after the full-relaxation of internal atomic positions and lattice parameters. In the fluorite structure, the lattice

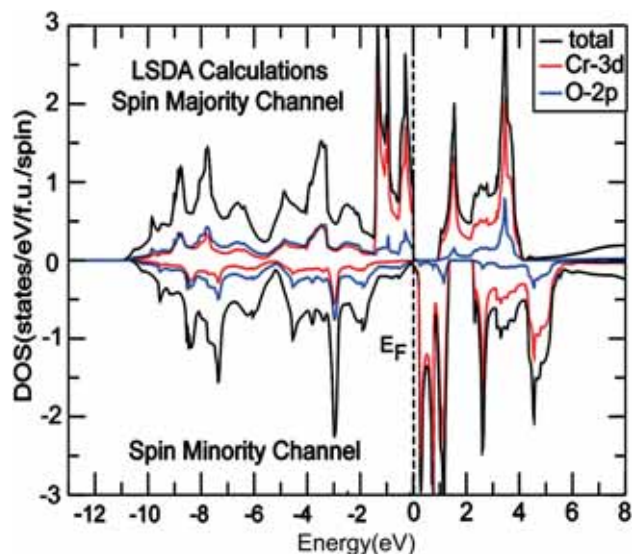


Figure 1. LSDA calculation for total (black), Cr-3d (red) and O-2p (blue) DOS of c-CrO₂. The system is metallic in the spin minority channel and insulating in the spin majority channel.

parameters used are $a = b = c = 4.334$ Å in the space group symmetry Fm-3m (no. 225). The Bravais lattice consists of one f.u. per unit cell. The positions of Cr and O atoms are taken at Cr: (0, 0, 0) and O: (0.25, 0.25, 0.25) [24]. Total ground-state energies (per f.u.) and magnetic moments as well as individual magnetic moments of Cr and O atoms were calculated both in LSDA and LSDA + U schemes. As the LMTO method gives accurate results for closely packed structure and as the structures under consideration is loosely packed, hence it is required to introduce empty spheres within the unit cell without hampering crystal symmetry. In this purpose, only a single empty sphere E was introduced. The muffin-tin radii (R_{MT}) of Cr, O and E are 2.20, 1.78 and 2.20 Å respectively.

3. Results and discussion

3.1 Electronic properties

Ferromagnetic spin polarized electronic structure calculations have been performed to elucidate the origin of MIT in c-CrO₂. Total ground-state energy, BS and DOS have been computed both in LSDA and LSDA + U treatments with increasing values of onsite Coulomb repulsion (U) to account the electron correlations in the later case, because it is very crucial for the description of ground-state electronic structure of c-CrO₂. The first attempt was to perform the DOS calculations both in LSDA and LSDA + U schemes. The total DOS per f.u., per Cr and O-sites in the LSDA approximations are represented by black, red and blue lines, respectively (see figure 1). The material is insulating in spin up channel, while spin down channel is metallic having minute charge contribution at E_F. It is evident from figure 1 that the contribution in the total DOS

near the close vicinity of Fermi level (E_F) is predominantly due to the Cr-3d character.

The e_g and t_{2g} bands are well separated in both spin channels. The centre of gravity of e_g bands is pushed just below the Fermi level (E_F), while the unoccupied t_{2g} bands are pushed above E_F by 0.96 eV. For spin up channel, e_g bands are found in the energy range -1.46 – 0 eV and t_{2g} bands are observed within the energy range 0.96 to 4.2 eV. As a result, a spin gap $\Delta \uparrow \sim 1$ eV is detected in this channel. This scenario occurs due to the broadening of Cr-3d bands slightly below E_F under high pressure situation resulting from collapse of volume by 7.3%.

In down spin channel, E_F is located within deep valley of a pseudo gap from which one can anticipate that only a small distortion to the crystal is sufficient to open a band gap at E_F . This can be achieved by applying even a small on-site Coulomb interaction (U). The e_g bands are observed in between -0.06 and 1.41 eV, while t_{2g} bands are observed within 2.25 to 5.75 eV resulting a spin gap $\Delta \downarrow \sim 0.84$ eV between them, hence they are well separated from each other. Hence, no band gap is found in the spin minority channel due to small but finite charge contribution at E_F . The system is thus nearly a half-metal. The scenario is completely different from t -CrO₂, in which the spin majority channel is metallic and minority spin channel is insulating. Nevertheless, Cr-3d e_g bands of c -CrO₂ are polarized just below and t_{2g} bands are polarized above E_F in the spin majority channel. The interaction between Cr-3d e_g and O-2p orbitals gives rise to mutual repulsion so that the occupied O-2p levels are pushed just below E_F , which results in a semi-conducting gap near E_F . However in down spin channel, both Cr-3d e_g and t_{2g} bands are polarized above E_F , but e_g bands have slight contribution below the Fermi level. The mutual interaction between Cr-3d e_g and O-2p orbitals push O-2p orbitals above E_F and connect the energetically lower lying states which are responsible for metallic nature. Partial band structures (PBS) have been calculated extensively to clarify the origin of this anomaly emerged out in the DOS calculations. The calculated PBS for c -CrO₂ in the LSDA treatment for majority spin channel are shown in figure 2a–c and for minority spin channel they are shown in figure 2d–f.

The Cr-3d e_g bands are observed in between the higher lying anti-bonding and lower lying bonding components of t_{2g} manifold due to tetrahedral crystal symmetry. The e_g bands are observed in the close vicinity of Fermi level due to the influence of cubic crystal field. It is revealed from the PBS calculations that, d_{xy} and d_{xz} states are exactly degenerate whose anti-bonding components are found well above E_F and a minute bonding components are found below E_F (see figure 2a). The d_{xz} orbital is found empty and shifted above E_F (figure 2b). The two e_g states ($d_{x^2-y^2}$ and $d_{3z^2-r^2}$) exactly degenerate and each of them is fully occupied and shifted just below E_F (see figure 2c) resulting in a spin gap between occupied e_g and unoccupied t_{2g} bands. The electrons in the e_g bands are almost localized. As a result, the material is semiconducting (having an energy gap ~ 0.84 eV) in the spin

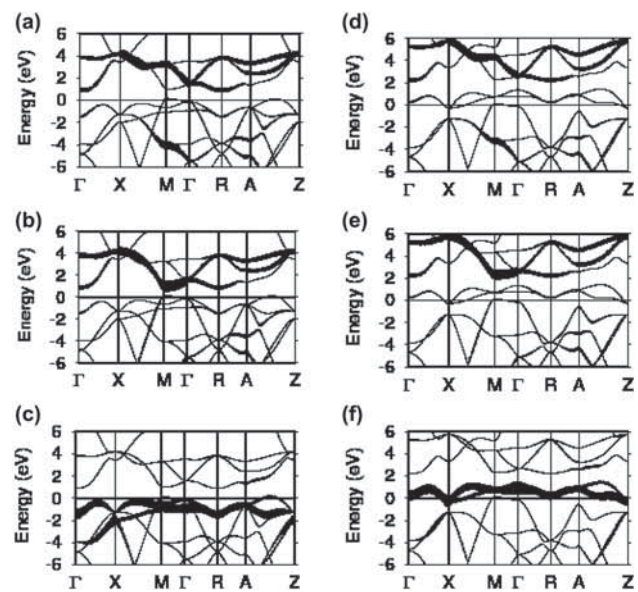


Figure 2. Calculated PBS of Cr-3d $_{xy/yz}$, d_{xz} and $d_{x^2-y^2}/3z^2-r^2$ states for up spin channel are represented in **a**, **b** and **c**, respectively. For down spin channel they are represented in **d**, **e** and **f**, respectively. The system is insulating in the up spin channel but metallic in the down spin channel. The p-d hybridization is predominantly due to the Cr-3d e_g orbitals. Zero in the energy axis represents Fermi level.

majority channel. The positions of the e_g orbitals towards the O-2p orbitals is exclusively responsible for the larger degree of p-d(e_g) hybridization, while p-d(t_{2g}) hybridization is insignificant. From the PBS calculations for spin minority channel, it is also clear that d_{xz} state is completely unoccupied (as shown in figure 2e), while d_{xy} and d_{yz} states also degenerate and their bonding components shifted below E_F while the anti-bonding components are far above E_F (see figure 2d). Eventually, neither $d_{x^2-y^2}$ nor $d_{3z^2-r^2}$ orbital is occupied, but they have very tiny charge contribution at E_F and they touch E_F which results in non-opening of band gap (see figure 2f). The system is thus metallic in this channel. The p-d(e_g) hybridization decreases dramatically which is evident from figure 2f.

Finally, LSDA + U calculations were performed with increasing values of U starting from 1 to 5 eV with constant value of $J = 0.85$ eV. The total ground-state energies, average DOS of Cr-3d and O-2p bands at E_F and band gaps calculated are summarized in table 1. The system becomes insulating at $U = 1$ eV but the band gap is very small ($E_g \sim 0.04$ eV). Higher values of U increase electron correlations for which occupied levels become more occupied and unoccupied states turn into more unoccupied, thereby broadening the band gap; what exactly happens in case of $U = 5$ eV (band gap $E_g \sim 1.05$ eV). Further, higher values of U were applied for the better realizations in the DOS, BS, ground-state energy and magnetic moment calculations. The calculated total DOS per f.u. (black), DOS of Cr-3d (red) and O-2p (blue) for c -CrO₂ with $U = 5$ are schematically shown in figure 3. The occupied Cr-3d e_g states are found

Table 1. Calculated total ground-state energies and magnetic moments, magnetic moments per Cr and O-site and total DOS (states/eV/f.u./spin) at E_F for Cr and O-sites in both spin channels for LSDA and LSDA + U schemes. Band gaps are also calculated for different U values.

Value of U (eV)	0	1	2	3	4	5
Total energy (eV)	−2399.03	−2399.04	−2398.95	−2398.89	−2398.89	−2398.86
Total mag. mom. (μ_B)	−1.99	−2.0	−2.0	−2.0	−2.0	−2.0
Cr-mag. mom. (μ_B)	−1.98	−1.93	−1.97	−2.0	−2.0	−2.0
O-mag. mom. (μ_B)	−0.009	−0.008	+0.016	+0.029	+0.042	+0.059
Band gap (eV)	0.0	0.04	0.13	0.42	0.72	1.05
Cr-3d DOS (up spin)	2.88	2.91	2.92	2.93	2.94	2.95
Cr-3d DOS (down spin)	1.05	1.02	0.99	0.96	0.93	0.90
O-2p DOS (up spin)	1.99	1.99	1.99	1.99	1.99	1.99
O-2p DOS (down spin)	2.05	2.05	2.04	2.04	2.04	2.05

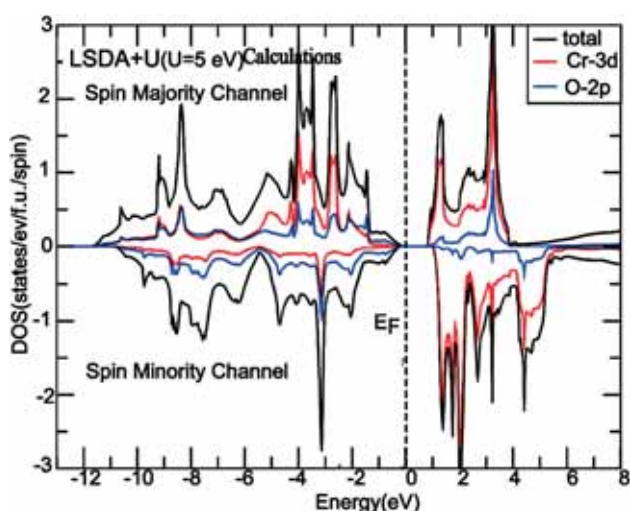


Figure 3. LSDA + U calculation for total (black), Cr-3d (red) and O-2p (blue) DOS of c-CrO₂ for $U = 5$ eV with $J = 0.85$ eV. The system becomes insulating with a band gap $E_g \approx 1.05$ eV.

in the energy range -6.0 to -1.32 eV for spin majority channel. Strong Coulomb repulsion increases orbital polarization which pushed the occupied e_g bands by ~ 0.36 eV below E_F . The unoccupied t_{2g} bands were found in between 0.89 to 3.90 eV and pushed down by 0.07 eV, which means occupancy of t_{2g} bands increases slightly and they move towards E_F which is also evident from PBS calculations (see figure 4a). Therefore, it is obvious that the application of U increases the occupancy of e_g levels significantly and hence localizes the e_g electrons. The occupied e_g levels are pushed well below E_F . The e_g and t_{2g} bands in the spin down channel are found in the energy range 1.08 to 2.40 eV and 2.40 to 6.03 eV, respectively, for $U = 5$ eV. Therefore the e_g bands are uplifted and touch t_{2g} bands. A band ~ 1.05 eV opens due to upward movement of e_g bands arising from spin polarization accompanied by strong electron correlation effect. As this MIT arises due to electron correlation, MIT in c-CrO₂ is Mott-Hubbard type.

The total DOS calculated at E_F per Cr site for $U = 0$ to 5 eV for spin majority channel are 2.88, 2.91, 2.92, 2.93, 2.94

and 2.95 (states/eV/f.u./spin), while the corresponding DOS calculated for spin minority channel are 1.05, 1.02, 0.99, 0.96, 0.93 and 0.90 (states/eV/f.u./spin). Therefore, DOS in the spin up channel increases, while it decreases in the down spin channel. The number of Cr-3d electrons for $U = 0$ to 5 eV are in increasing order (see table 1), which indicates that the application of U enhances the orbital polarization due to strong electron correlation effect and localizes the itinerant d-electrons. The occupancy of each e_g orbital increases and is shifted below the Fermi level. The t_{2g} bands remain unoccupied and are shifted above E_F . The e_g bands in down spin channel are polarized above E_F such that spin gap between e_g and t_{2g} bands diminishes. As a result, a gap of $E_g \sim 1.05$ eV for $U = 5$ eV is detected near E_F . It is also found that the total O-2p DOS at E_F is constant both in spin up (1.99 states/eV/f.u./spin) and spin down channels (2.04 states/eV/f.u./spin). Therefore, O-2p electrons have no role in the observed MIT.

To elucidate the MIT in c-CrO₂, PBS have also been calculated for $U = 5$ eV (see figure 4). The two t_{2g} orbitals d_{xy} and d_{yz} are also degenerate in the spin up channel (see figure 4a). Their unoccupied anti-bonding components are pushed above and minute occupied bonding components are pushed well below E_F . The rest t_{2g} orbital (d_{xz}) is found completely unoccupied (figure 4b). Both $d_{x^2-y^2}$ and $d_{3z^2-r^2}$ states are fully occupied and shifted well below E_F (figure 4c) and hybridized with O-2p orbitals. This hybridization is stronger than that observed in LSDA calculations; therefore strength of FM increases in LSDA + U treatment. The electron occupancy of all the occupied states increases due to the strong electron correlation effect. In down spin channel, d_{xy} and d_{yz} states are also degenerate and have unoccupied anti-bonding components, while their bonding components have very small contribution below E_F (as shown in figure 4d). The d_{xz} state is found unoccupied and is pushed above E_F . Dramatic change in the occupancy of e_g orbitals is noticed in the PBS calculations for LSDA + U treatment. The e_g orbitals are polarized above E_F due to strong electron correlation effect. As a consequence, a band gap is observed in down spin

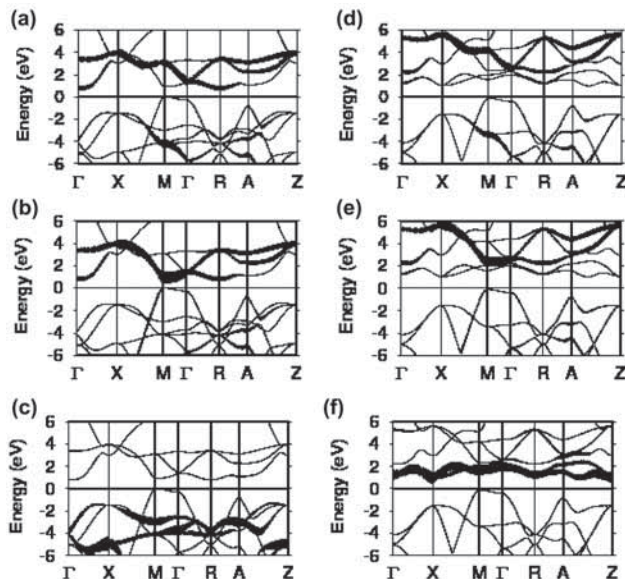


Figure 4. Calculated LSDA + U PDOS for $U = 5$ eV of Cr-3d_{xy/yz}, d_{x²-y²} and d_{3z²-r²} states for up spin channel are represented in **a**, **b** and **c**, respectively. For down spin channel they are represented in **d**, **e** and **f**, respectively. The compound is insulating in both spin channels. The p-d hybridization in the spin majority channel increases significantly. Zero in the energy axis represents Fermi level.

channel (figure 4f), which is responsible for MIT in c-CrO₂. Therefore, Coulomb correlation plays crucial role in the MIT in c-CrO₂.

3.2 Magnetic properties

The next effort was given to investigate the magnetic behaviour of c-CrO₂ for both LSDA and LSDA + U treatments. In the LSDA + U treatment, a series of on-site Coulomb interactions starting from $U = 1$ to 5 eV were tested which is well agreement with other reports [37,38]. In the present study, the total ground-state energies, magnetic moments per f.u., magnetic moment per Cr and O-atom are summarized in table 1 for both LSDA and LSDA + U schemes. It is evident from the calculations that the contributions to the total magnetic moments arise entirely from Cr-magnetic moments rather than O-magnetic moments.

Applications of higher value of U results in strong electron polarizations, for which Cr- e_g states become fully occupied and are pushed well below the Fermi level. Subsequently, the hybridization between occupied Cr- e_g and O-2p orbitals increases remarkably that is responsible for strong FM of c-CrO₂. Further, due to strong electron polarization arising from electron correlation effect, two electrons in the e_g states (d_{x²-y²} and d_{3z²-r²}) aligned perfectly parallel to each other which is responsible for higher Cr-magnetic moments. Therefore, it is obvious that high U values result in high Cr-magnetic moments. The calculated magnetic moment per Cr atom for LSDA scheme is $-1.98 \mu_B$ which gradually increases

with U . The calculated total magnetic moments per formula unit (f.u.) and average magnetic moments of Cr and O sites obtained from the LSDA and LSDA + U treatments in the cubic structure of CrO₂ are reported in table 1. It is evident from table 1 that the total magnetic moment per f.u. remains constant ($-2.0 \mu_B$) for all values of U , although the average Cr-magnetic moment increases with increasing values of U . The average magnetic moments per O-site are -0.009 and $-0.008 \mu_B$ for $U = 0$ and 1 eV, respectively, which means Cr and O sites are weakly positively coupled; thereby, p-d hybridizations are weaker compared to higher U values, wherein anti-coupling of Cr and O sites are in increasing order which indicates increasing of admixture between them resulting strong O-2p-Cr-3d hybridizations. These p-d hybridizations are further responsible for the FM behaviour of CrO₂ in the cubic CaF₂-type structure. It is also obvious that the strength of FM increases in the LSDA + U calculations due to the strong correlations effect. Magnetic moments of O-sites increase gradually with U , which reflects increasing of Cr-O anti-coupling. Any two Cr-atoms are connected via an oxygen atom which is further anti-coupled with Cr-atoms. Therefore, double exchange mechanism arising from strong Hund's coupling is responsible for observed FM of c-CrO₂.

4. Conclusions

In conclusion, it is observed that CrO₂ in the cubic CaF₂-type structure is a FM nearly half-metal in the LSDA approach. In this treatment, the spin majority channel is insulating due to downward shifting of almost occupied d_{x²-y²} and d_{3z²-r²} bands just below E_F and upward lifting of unoccupied t_{2g} bands. The e_g bands in the down spin channel have small but finite contribution of charges at E_F , for which no band gap opens and the system is thus metallic. The t_{2g} bands are unoccupied in this case. The material encounters MIT upon the application of Coulomb repulsion $U = 1$ eV. Application of U increases the electron correlation which enhances orbital polarization, as a result, e_g orbitals in the spin majority channel are polarized far below and t_{2g} orbitals are polarized far above E_F resulting in broadening of spin gap. In the spin down channel, the e_g orbitals are polarized well above the Fermi level and touch the empty t_{2g} orbitals causing opening of a band gap in the vicinity of E_F . The applications of larger U broaden the gap. Coulomb repulsion increases hybridization between occupied Cr-3d e_g and O-2p orbitals, which is responsible FM in the insulating phase of c-CrO₂. Higher value of U increases the strength of FM. Thus Coulomb repulsion is the key element for MIT in c-CrO₂.

References

- [1] Soulen R J, Byers J M, Osofsky M S, Nadgorny B, Ambrose T, Cheng S F *et al* 1998 *Science* **282** 85
- [2] Li X W, Gupta A and Xiao G 1999 *Appl. Phys. Lett.* **75** 713

- [3] Stagaescu C B, Su X, Eastman D E, Altmann K N, Himpfel F J and Gupta A 2000 *Phys. Rev. B* **61** R9233
- [4] Fang F Y, Chien C L, Ferrari E F, Li X W, Xiao G and Gupta A 2000 *Appl. Phys. Lett.* **77** 286
- [5] Ji Y, Strijkers G J, Yang F Y, Chien C L, Byers J M, Anguelouch A *et al* 2001 *Appl. Phys. Lett.* **86** 5585
- [6] Coey J M D and Venkatesan M 2002 *J. Appl. Phys.* **91** 8345
- [7] Moodera J S, Kinder L R, Wong T M and Meservey M 1995 *Phys. Rev. Lett.* **74** 3273
- [8] Gupta A, Li X W and Xiao G 2001 *Appl. Phys. Lett.* **78** 1894
- [9] Dai J and Tang J 2001 *J. Phys. Rev. B* **63** 054434
- [10] Hwang H Y, Cheong S W, Ong N P and Batlogg B 1996 *Phys. Rev. Lett.* **77** 2041
- [11] Manoharan S S, Elefant D, Reiss G and Goodenough J B 1998 *Appl. Phys. Lett.* **72** 984
- [12] Coey J M D, Berkowitz A E, Balcells L, Putris F and Berry A 1998 *Phys. Rev. Lett.* **80** 3815
- [13] Mazin I I, Singh D J and Ambroasch-Draxl C 1999 *Phys. Rev. B* **59** 411
- [14] Kunes J, Novak P, Oppeneer P M, König C, Fraune M, Rüdiger U *et al* 2002 *Phys. Rev. B* **65** 165105
- [15] Toropova A and Kotliar G 2005 *Phys. Rev. B* **71** 172403
- [16] Dedkov Y S, Vinogradov A S, Fonin M, König C, Vyalikh D V, Preobrajenski A B *et al* 2005 *Phys. Rev. B* **72** 060401(R)
- [17] Kanchana V, Vaitheeswaran G and Alouan M 2006 *J. Phys. Condens. Matter.* **18** 5155
- [18] Chioncel L, Allmaier H, Arrigoni E, Yamasaki A, Daghofer M, Katsnelson M I *et al* 2007 *Phys. Rev. B* **75** 140406(R)
- [19] Singh G P, Ram S, Eckert J and Fecht H J 2009 *J. Phys. Conf. Ser.* **144** 012110
- [20] Anwar M S, Czeschka F, Hesselberth M, Porcu M and Aarts J 2010 *Phys. Rev. B* **82** 100501(R)
- [21] Wu H Y, Chen Y H, Deng C R and Su X F 2012 *Int. J. Modern Phys. B* **15** 1250091
- [22] Singh A, Voltan S, Lahabi K and Aarts J 2015 *Phys. Rev. X* **5** 021019
- [23] Maddox B R, Yoo C, Kasinathan D, Pickett W and Scalettar R 2006 *Phys. Rev. B* **73** 144111
- [24] Srivastava V, Rajagopalan M and Sanyal S P 2008 *Eur. Phys. J. B* **61** 131
- [25] Dho J, Ki S, Gubkin A, Park J and Sherstobitova E 2010 *Solid State Commun.* **150** 1
- [26] Kim S, Kim K, Kang C J and Min B I 2012 *Phys. Rev. B* **85** 094106
- [27] Wu H, Chen Y, Deng C and Su X 2012 *Phase Transit.* **85** 8
- [28] Li Y and Hao J 2012 *Solid State Commun.* **152** 1216
- [29] Alptekin S 2015 *J. Mol. Model* **21** 304
- [30] Hohenberg P and Kohn W 1964 *Phys. Rev. B* **136** B864
- [31] Kohn W and Sham L J 1965 *Phys. Rev. B* **140** A1133
- [32] Anderson O K 1975 *Phys. Rev. B* **12** 3060
- [33] Perdew J P and Wang Y 1992 *Phys. Rev. B* **45** 13244
- [34] Anderson O K and Jepsen O 1984 *Phys. Rev. Lett.* **53** 2571
- [35] Anisimov V I, Aryastawan F and Lichtenstein A I 1997 *J. Phys.: Condens. Matter* **9** 767
- [36] Anisimov V I, Zaanen J and Anderson O K 1991 *Phys. Rev. B* **44** 943
- [37] Korotin M A, Anisimov V I, Khomskii D I and Sawatzky G A 1998 *Phys. Rev. Lett.* **80** (N19) 4305
- [38] Matej K, Claude E and Manfred F 2004 *Phys. Rev. B* **69** 132409